Binding energy of bound excitons D^0X in quantum wells

J. L. Dunn, C. A. Bates, and M. J. Pye
Department of Physics, University of Nottingham, University Park, Nottingham NG7 2RD, United Kingdom

D. Boffety,* A.-M. Vasson,*† A. Vasson,* and J. Leymarie*
LASMEA, Physique 4, Université Blaise Pascal Clermont II, Complexe Scientifique des Cézeaux, 24 Avenue des Landais, 63177 Aubiere, France

(Received 3 March 1998)

The binding energies of excitons bound to silicon donors in GaAs/$Ga_{1-x}Al_xAs$ quantum-well (QW) structures have previously been investigated experimentally as a function of the well width by several groups. The most comprehensive data show a clear maximum for a well width of about 100 Å, and a steady decrease for widths above this. Existing theories give qualitative agreement with the decrease in binding energy with increasing well width. However, no theory predicts a maximum near 100 Å. Furthermore, the quantitative agreement is poor for all well widths. We develop a theoretical model using a density-functional approach which correctly predicts the maximum in the binding energy at 100 Å. The agreement with the experimental results is significantly better for all well widths than that of existing models. Photoluminescence experiments have also been carried out on samples with a wide range of different doping profiles in order to clarify the previous experimental results and provide additional information on the effect of the position of the impurity in the QW. [S0163-1829(98)05036-X]

I. INTRODUCTION

Much experimental data exists on the donor-bound exciton (D^0X) in GaAs/$Ga_{1-x}Al_xAs$ quantum wells (QWs). Several investigations have centered on the variations of the binding energy E_{XD} as a function of the well width d for both single QWs (Ref. 1) and multiple QWs,[2,3] as summarized in Ref. 4. The most comprehensive results are those of Reynolds *et al.*,[3] who investigated impurities both at the center and edge of a QW in multiple-quantum-well samples with an aluminum concentration $x=0.25$. Their results exhibit a clear maximum in the E_{XD}-d curve for $d=100$ Å. Above this the binding energy steadily decreases. The results of Refs. 1 and 2 are approximately 0.2–0.3 meV lower than those of Ref. 3, although insufficient samples were included to make any clear deductions on the variation with d. It is not clear how much of this difference is due to differing sample characteristics; the aluminum concentration x is 0.22 in Ref. 1, and is not specified in Ref. 2.

The first theoretical calculations of the D^0X binding energy in quantum wells were by Kleinman,[5] who used a six-parameter wave function to determine the energy variationally using a two-dimensional model. However, it was necessary to include an artificial nonvariational parameter in order to obtain bound states, and the results did not exhibit a turning point in the binding energy. Haufe[6] then calculated the binding energy for the finite barrier problem using a variational approach within a density-functional formalism. These results show a possible maximum around 60 Å, but this is not as clear as it is at the lower limit of their calculations. Very recently, Liu and Kong[4] carried out variational calculations using a two-parameter wave function for impurities at the center and edge of a QW incorporating interparticle correlation effects, for values of d varying between 8 and 150 Å. A clear maximum in E_{XD} was found, but at a value of about 15 Å rather than 100 Å. This is much smaller than that observed experimentally. Also, the magnitude of the binding energy and its variation with well width only give qualitative agreement with the available experimental data.

The purpose of this paper is to describe details of a theoretical model involving a nonvariational approach to density-functional theory. Photoluminescence experiments have also been undertaken on samples with a range of doping profiles in order to investigate the dependence of the binding energy upon the positions of the impurities in the wells, and also to help clarify the previous experimental picture. We use molecular-beam-epitaxy-grown GaAs/$Ga_{1-x}Al_xAs$ QW samples with $x=0.33$, well widths d in the range 75–170 Å, and barriers sufficiently wide to prevent interaction between impurity centers. The experimental and theoretical values are compared with each other and with the previously published values. Our experimental results are found to be very close to those of Ref. 3 for all well widths, even though the latter are for $x=0.25$ and with barriers of only 100 Å. Both sets of results exhibit a pronounced maximum at around 100 Å. Our theory correctly predicts a maximum at this position. Also, the magnitudes of binding energies predicted agree well with the experimental values at all well widths, and are considerably better than those of the previous theories.

Section II describes the results obtained from the experiments. Sections III–V give some background details of density-functional theory and how it may be applied to the D^0X system. Section VI describes the calculation of the total energy of the system, and Sec. VII compares our results with the original and current experimental data and the previous theoretical calculations. A preliminary report of this work was presented by Pye *et al.*[7]

II. EXPERIMENTAL DETAILS

Optical spectroscopy experiments have been carried out on silicon-doped GaAs/$Ga_{0.67}Al_{0.33}As$ multiple-QW samples of between 30 and 150 periods, and also on a single-QW sample. The samples were grown at Nottingham using a Varian GEN II molecular-beam-epitaxy machine on a semi-insulating GaAs substrate followed by a pure GaAs buffer layer. The well widths were in the range 75–170 Å. Some samples were uniformly doped, either across the whole well or in the central third, with a silicon concentration of 10^{16} cm^{-3}. Samples with δ-doping at various positions in the QW to a Si concentration of 10^{10} cm^{-2} (or 2.5×10^{10} cm^{-2} in one sample) were also investigated. One sample was also constructed with the central third Si doped as above, and with the outer thirds doped with a lower Si concentration of 2×10^{14} cm^{-3}. The barrier layers were arranged to be sufficiently thick that the ground-state wave function in one well has little overlap with those in adjacent wells.

Photoluminescence (PL) experiments were carried out at very low temperatures using an excitation from the 5145-Å line of a cw argon-ion laser. The emitted photons were analyzed through a grating monochromator of focal length 0.64 m, and detected after standard lock-in amplification by a liquid-nitrogen-cooled Ge detector. Both the free-exciton transition energy X_{e1hh1} and the D^0X transitions have also been observed in the single QW sample by thermally detected optical absorption and by reflectivity. The identification of the X_{e1hh1} and D^0X PL recombination peaks were checked using temperature-dependent (4–300 K) and excitation-intensity-dependent PL experiments. The δ-doped multiple-quantum-well samples in which the silicon atoms were positioned away from the QW center have given estimates of the decrease of E_{XD} when the doping position moves from the center to the edge of the QW. This decrease depends upon the QW thickness; the magnitude is ~0.3 Å (in wavelength units) for a well of thickness 100 Å, and 0.5 Å for a well of thickness 170 Å, in agreement with Reynolds *et al.*[3] In samples of uniformly doped wells, the D^0X transitions energies are identical to those in samples with δ-doping at the center of the well, and therefore can be assumed to arise from Si atoms at the center of the QW. Some typical PL spectra are given in Fig. 1. The D^0X feature shown consists of a double line from Si atoms located at the center (lower energy) and an edge of the well (higher energy). Figure 2 shows the measured binding energies (●) of the D^0X center as a function of the QW thickness. The results of Ref. 3 (○) are also shown for comparison. It can be seen that both sets of measurements are very similar, despite the slightly different sample characteristics. In particular, the maximum in the binding energy for a QW of width of about 100 Å is clear in both sets of results. The results of Refs. 1 and 2 are not given in this figure, although a comparison of them and the results of Ref. 3 can be found in Ref. 4.

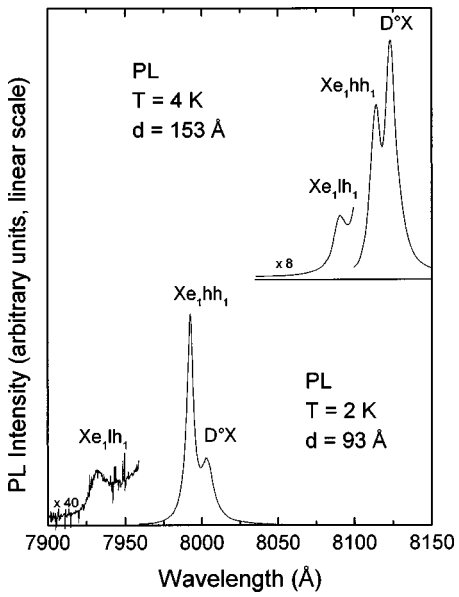

FIG. 1. The PL spectra from two samples; one is from a GaAs/$Ga_{0.67}Al_{0.33}As$ sample in which there is one QW with $d=93$ Å and the other relates to a similar sample containing 150 QWs with $d=153$ Å. The peaks labeled X_{e1lh1} and X_{e1hh1} correspond to free-exciton transitions, and the D^0X peak is the recombination of the neutral bound exciton.

III. DENSITY-FUNCTIONAL THEORY

A. Review and background

Treatment of the D^0X problem is intrinsically difficult because it is necessary to specify the positions of three particles. A strict variational calculation requires a minimum of three variational parameters and evaluation of three Hartree terms. An alternative approach is to use density-functional theory, which is a variational-type method tailored specifically to many-body systems. Its roots lie in the Thomas-Fermi method of treating an inhomogeneous electron gas. Hohenberg and Kohn[8] showed that all aspects of the electronic structure of a system in its ground state may be described by the electron density. Using this work as a basis, Kohn and Sham[9] were able to formulate a particularly useful form of density-functional theory involving single-particle equations to be solved self-consistently. Density-functional theory is an attractive approach as it includes both exchange and correlation effects (albeit approximately) while maintaining the simplicity of self-consistent equations.

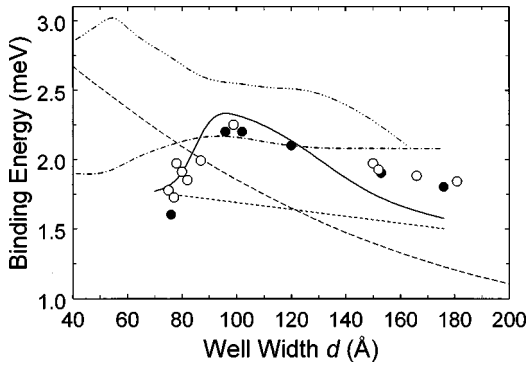

FIG. 2. The binding energy E_{XD} for a D^0X center at the center of a $Ga_{1-x}Al_xAs$ single QW a function of the QW width d. The solid points ● are the current experimental values, and the solid line is the current theoretical calculation (both for $x=0.33$). Also shown are the experimental results of Ref. 3 (○) and the theoretical results of Refs. 5 (short dash), 4 (long dash, $x=0.25$), and 6 (– –, $x=0.4$; —·—·—·—, $x=0.2$).

Density-functional theory has been applied to the D^0X system in bulk semiconductors by a number of authors,[10–14] and generally good agreement with experiment has been obtained. More recently, Xia and Quinn[15] used density-functional theory to calculate the binding energies of D^- centers in quantum wells subject to a magnetic field. It is expected that, for a multiparticle theory of this type, relatively greater accuracy will result as the number of particles in the complex increases. Thus an improvement in the relative accuracy is expected by moving from the two-particle complex, as studied by Xia and Quinn,[15] to the three-particle D^0X complex. As mentioned earlier, Haufe[6] used a density-functional formalism to study the D^0X center, but only within a variational ansatz. In the following analysis, we will employ the full multicomponent form of the Kohn-Sham equations within the local-density approximation.

B. Application to D^0X in a QW

The D^0X system involves two electrons and a hole. As wide barriers were present in the samples studied, penetration into other wells is negligible, and we can model the system in terms of a single quantum well. For simplicity, the hydrogenic impurity ion will be assumed to be located at the center of the quantum well. Therefore for each particle, the QW potential is

$$V_{\mathrm{QW},\alpha}(z)=\begin{cases}0 & \text{if } -d/2<z<d/2\\ V_{0,\alpha} & \text{otherwise,}\end{cases} \tag{3.1}$$

where $\alpha=e$ and h for an electron and hole, respectively. The z axis is chosen to lie along the direction of growth. For $Ga_{1-x}Al_xAs/GaAs$ materials,[15] the gap mismatch is $\Delta E_g=1.247x$ eV, and the barrier heights are $V_{0,e}=0.65\Delta E_g$ and $V_{0,h}=0.35\Delta E_g$.

It is necessary to consider the Coulomb interactions between the two electrons and also between the electron and the hole; also the exchange-correlation potential $V_{\mathrm{xc},\alpha}[n_e,n_h]$, which are functionals of the electron and hole densities n_e and n_h, must be introduced. The precise forms of these functionals will be discussed shortly. The effective Hamiltonian for one of the single particles in the Kohn-Sham basis is given by

$$\mathcal{H}_{\mathrm{eff},\alpha}=\left[-\frac{m_e}{m_\alpha}\nabla^2+V_{\mathrm{QW},\alpha}(z)+V_{\mathrm{eff},\alpha}(\rho,z)\right], \tag{3.2}$$

where m_α are the electron and hole effective masses, distances are given in terms of the effective Bohr radius a_0 $(=4\pi\epsilon\hbar^2/m_ee^2)$ and energy in terms of the effective Rydberg $R(=m_ee^4/2\hbar^2(4\pi\epsilon)^2)$, and where ϵ is the background dielectric constant. In Eq. (3.2), the effective potential $V_{\mathrm{eff},\alpha}(\rho,z)$ in polar coordinates (ρ,z) for particles at $\mathbf{r}$ and $\mathbf{r}'$ is

$$V_{\mathrm{eff},\alpha}(\rho,z)=\sum_{\beta=e,h}\int dr'\,u_{\alpha\beta}(\mathbf{r}-\mathbf{r}')n_\beta(\mathbf{r}')$$
$$+V_{\mathrm{xc},\alpha}[n_e,n_h]\mp\frac{1}{\sqrt{\rho^2+z^2}}, \tag{3.3}$$

where

$$u_{\mathrm{ee}}=\frac{+1}{|\mathbf{r}-\mathbf{r}'|},$$

$$u_{\mathrm{eh}}=u_{\mathrm{he}}=\frac{-1}{|\mathbf{r}-\mathbf{r}'|}\quad\text{or}\quad u_{\mathrm{hh}}=0. \tag{3.4}$$

The first term on the right-hand side represents the Coulomb interaction between the particles, and the last term represents the interaction between the particle and the impurity center; the minus sign applies to the electron and the positive sign to the hole.

In general, the Kohn-Sham equations are of the form

$$\mathcal{H}_{\mathrm{eff},\alpha}\Psi_{i,\alpha}(\rho,z)=\epsilon_{i,\alpha}\Psi_{i,\alpha}(\rho,z), \tag{3.5}$$

where $\Psi_{i,\alpha}(\rho,z)$ are a set of single-particle wave functions, and $\epsilon_{i,\alpha}$ the corresponding energy levels. The ground-state particle densities are then written in the form

$$n_\alpha(\rho,z)=\sum_i|\Psi_{i,\alpha}(\rho,z)|^2, \tag{3.6}$$

where the sum is carried out over all the occupied single-particle states. For the ground state of the D^0X complex, there is only one single-particle state occupied for each particle (the two electrons are in their lowest-energy states with opposing spins). Consequently, the index i is superfluous here and will be subsequently omitted.

C. Exchange-correlation potential

To solve the Kohn-Sham equations, a form for the exchange-correlation potential is needed. We thus follow Wunsche and Henneberger,[12] who derived simple forms for the exchange-correlation potential using the local density and Slater approximations (as discussed in Ashcroft and Mermin,[16] for example). They applied their potentials to the D^0X system in bulk semiconductors by writing the exchange-correlation contribution to the total energy, in dimensionless units, as

$$E_{\mathrm{xc}}[n_e(\mathbf{r}),n_h(\mathbf{r})]=\int d^3\mathbf{r}\;\varepsilon_{\mathrm{xc}}[n_e(\mathbf{r}),n_h(\mathbf{r})], \tag{3.7}$$

where

$$\varepsilon_{\mathrm{xc}}[n_e(\mathbf{r}),n_h(\mathbf{r})]=\varepsilon_x[n_e(\mathbf{r}),n_h(\mathbf{r})]+\varepsilon_c[n_e(\mathbf{r}),n_h(\mathbf{r})],$$

with

$$\varepsilon_x[n_e,n_h]=-1.1545\left(n_e\left[\frac{n_e}{N_e}\right]^{1/3}+n_h\left[\frac{n_h}{N_h}\right]^{1/3}\right), \tag{3.8}$$

and

$$\varepsilon_c[n_e,n_h]=-\beta_en_e^{7/6}-\beta_hn_h^{7/6}-\beta_{\mathrm{eh}}(n_en_h)^{7/12}. \tag{3.9}$$

N_e and N_h are the total numbers of electrons and holes in the system (2 and 1, respectively, for D^0X). The coefficients in Eq. (3.9) are defined by

$$\beta_e=\beta_s(N_e),\quad \beta_h=\beta_s(N_h)\sqrt{1+1/\sigma}, \tag{3.10}$$

and

$$\beta_{\rm eh}=0.761\left[0.8+0.2\left(\frac{[1+\sigma^2]}{2\sigma}\right)^{1/2}\right]-\beta_e-\beta_h, \quad (3.11)$$

where

$$\beta_s(N_\alpha)=\begin{cases}0.0985 & \text{if } N_\alpha=1\\ 0.1480 & \text{if } N_\alpha>1,\end{cases} \quad (3.12)$$

and where $\sigma=m_e/m_h$ is the mass ratio.

The above results arise from applying to nonuniform systems the result which would be obtained by treating the electrons and holes as free particles. Wunsche and Henneberger[12] calculated the correlation energy by interpolating the fit between the limiting cases of a *single-component* plasma obtained in Ref. 17.

The exchange-correlation potentials can then be found from

$$V_{{\rm xc},\alpha}[n_e,n_h]=\frac{\delta E_{\rm xc}[n_e,n_h]}{\delta n_\alpha(\mathbf{r})}. \quad (3.13)$$

This gives

$$V_{{\rm xc},e}[n_e,n_h]=-1.2218n_e^{1/3}-1.1667\beta_e n_e^{1/6}-0.5833\beta_{\rm eh}n_e^{-5/12}n_h^{7/12} \quad (3.14)$$

and

$$V_{{\rm xc},h}[n_e,n_h]=-1.5393n_h^{1/3}-1.1667\beta_h n_h^{1/6}-0.5833\beta_{\rm eh}n_e^{7/12}n_h^{-5/12}. \quad (3.15)$$

In this calculation, spin effects are not included. We consider only the case of zero magnetic field so that spin only plays a part in the correlation energy of the system. As the theoretical work on the D^0X system in bulk semiconductors cited above has produced accurate results while omitting the spin dependence, it therefore appears likely that spin effects will cause only a minor correction for the QW case. However, we note that spin could be included in our calculation above through the use of spin-density-functional theory. The latter requires the use of the spin-up and spin-down densities for each of the particles by the simple formula $n_\alpha=n_\alpha\uparrow+n_\alpha\downarrow$. Here this would necessitate working with four single-particle equations rather than two.

Self-interaction effects have been considered by Xia and Quinn[15] in their study of the D^- center in a quantum well in a magnetic field. They adopted the treatment of Perdew and Zunger[18] by adapting their exchange-correlation potential to compensate for the imperfect cancellation between the self-Coulomb and self-exchange terms. As Perdew and Zunger[18] estimated that over 90% of the self-interaction terms mutually cancel each other for the bulk case, they will be neglected entirely here.

IV. SOLUTION OF THE KOHN-SHAM EQUATIONS BY AN EXPANSION TECHNIQUE

The effective Hamiltonian $\mathcal{H}_{{\rm eff},\alpha}$ for each component α can be decomposed into two parts:

$$\mathcal{H}^{(a)}_{{\rm eff},\alpha}(z)=\frac{-m_e}{m_\alpha}\frac{d^2}{dz^2}+V_{{\rm QW},\alpha}(z) \quad (4.1)$$

and

$$\mathcal{H}^{(b)}_{{\rm eff},\alpha}(\rho,z)=\frac{-m_e}{m_\alpha}\nabla_\rho^2+V_{{\rm eff},\alpha}(\rho,z) \quad (4.2)$$

$\mathcal{H}^{(a)}_{{\rm eff},\alpha}(z)$ is the Hamiltonian of the component of type α in its respective quantum well. The solution of this Hamiltonian is straightforward, and is discussed later. We denote the subband wave functions and energies resulting from such a solution by $\xi_{\alpha,n}(z)$ and $E_{\alpha,n}$, respectively, where $n=1,2,\ldots$. $\mathcal{H}^{(b)}_{{\rm eff},\alpha}(\rho,z)$ is the part of the effective Hamiltonian which couples the subband wave functions.

In order to proceed, the single-particle wave function Ψ_α with angular momentum quantum number m is expanded in terms of the subband wave functions as

$$\Psi_\alpha\equiv\psi_{\alpha,m}(\rho,\theta,z)=\frac{1}{\sqrt{2\pi}}e^{im\theta}\sum_{n=1}^{+\infty}\frac{\phi_{\alpha,m,n}(\rho)}{\sqrt{\rho}}\xi_{\alpha,n}(z), \quad (4.3)$$

where θ is the polar angle in the x-y plane. The Kohn-Sham equations then become

$$\left[-\frac{m_e}{m_\alpha}\frac{d^2}{d\rho^2}+\frac{m_e}{m_\alpha}\frac{m^2-\frac{1}{4}}{\rho^2}-\epsilon_\alpha+E_{\alpha,n}\right]\phi_{\alpha,m,n}(\rho)+\sum_{n'=1}^{+\infty}\nu^{nn'}_{{\rm eff},\alpha}\phi_{\alpha,m,n}(\rho)=0, \quad (4.4)$$

where the effective potentials in the coupling term are given by

$$\nu^{nn'}_{{\rm eff},\alpha}(\rho)=\int\xi_{\alpha,n}(z)V_{{\rm eff},\alpha}(\rho,z)\xi_{\alpha,n'}(z)dz. \quad (4.5)$$

Here only the ground state is considered, for which $m=0$. Hence the index will subsequently be dropped from the equations.

The coupling term in the effective Hamiltonian mixes the subband functions, so that Eq. (4.4) is a set of coupled second-order differential equations. It is clear that the potential depends upon the densities themselves, so that the procedure adopted for solving the coupled equations must be self-consistent. In order to produce a solution, boundary conditions at $\rho=0$ and at $\rho=\infty$ must be imposed; these will be discussed in Sec. V.

In order to simplify the problem, we retain one term only in the subband summation (and so subsequently omit the index n). For each step in the self-consistent calculation, the equation to be solved is then a second-order eigenvalue equation. Our justification for this comes from the work of Xia and Quinn,[15] who investigated the effect of coupling in the energy subbands for D^- centers for QWs having a width comparable to the effective Bohr radius (i.e., for GaAs, $d\sim100$ Å). For wells of this size, the spacing between the energy subbands is at least an order of magnitude larger than the other energy terms in the equation, and thus we would expect only a small amount of subband coupling here. Xia and Quinn[15] performed two sets of calculations: in the first set, they included several subbands in the summation from Eq. (4.4), while, in the second set, they included only one

subband. Their results showed a difference of less than 0.1% in the final energy. The coupling of the hole subbands is likely to be slightly larger than that of the electrons as the quantum-well potential for the holes is shallower; nonetheless, it seems highly unlikely that this will lead to a significant discrepancy in the final result.

V. SOLUTION OF THE QUANTUM-WELL HAMILTONIAN

The expansion technique requires the effective Hamiltonian to be separated into two parts. We first solve the part which represents the quantum-well confinement. In dimensionless units, the quantum-well equations are

$$-\frac{m_e}{m_\alpha}\frac{d^2\xi_\alpha(z)}{dz^2}+V_{\mathrm{QW},\alpha}(z)\xi_\alpha(z)=E_\alpha\xi_\alpha(z). \tag{5.1}$$

The (un-normalized) ground-state solution to Eq. (5.1) is well known; it is given here by

$$\xi_\alpha(z)=\cos(k_\alpha z) \quad \text{for } |z|<\frac{d}{2},$$

and (5.2)

$$\xi_\alpha(z)=B_\alpha\exp(-\kappa_\alpha|z|) \quad \text{for } |z|>\frac{d}{2},$$

where

$$k_\alpha=(m_\alpha E_\alpha/m_e)^{1/2} \quad \text{and} \quad \kappa_\alpha=(m_\alpha(V_{0,\alpha}-E_\alpha)/m_e)^{1/2}. \tag{5.3}$$

Here E_α and B_α are determined by ensuring continuity of $\xi_\alpha(z)$ and its first derivative at the edges of the well.

The asymptotic forms for the function $\phi_\alpha(\rho)$ at the ends of the ranges of integration of the differential equation (4.4) must be specified. In order to solve the eigenvalue equations, it is necessary to know the asymptotic behavior of $[d^2\phi_\alpha(\rho)/d\rho^2]$ and $[1/\phi_\alpha(\rho)][d\phi_\alpha(\rho)/d\rho]$ to define the eigenvalue equation. For a physically valid solution, the particle density $n_\alpha(r)$ must remain finite throughout the range of integration. As $\rho\to 0$, the dominant term in the differential equation is $-1/(4\rho^2)$, so that the differential equation becomes

$$\left[-\frac{d^2}{d\rho^2}-\frac{1}{4\rho^2}\right]\phi_\alpha(\rho)=0. \tag{5.4}$$

This can be solved exactly; its general solution is

$$\phi_\alpha(\rho)=c_1\sqrt{\rho}(1+c_2\ln(\rho)), \tag{5.5}$$

where c_1 and c_2 are arbitrary constants. As the solutions must remain finite, then $c_2=0$. Therefore,

$$\frac{1}{\phi_\alpha(\rho)}\frac{d\phi_\alpha(\rho)}{d\rho}\to\frac{1}{2\rho} \quad \text{as } \rho\to 0. \tag{5.6}$$

As $\rho\to\infty$, only the constant terms remain, so that the differential equation becomes

$$\left[-\frac{m_e}{m_\alpha}\frac{d^2}{d\rho^2}-\epsilon_\alpha+E_\alpha\right]\phi_\alpha(\rho)=0, \tag{5.7}$$

and has a solution

$$\phi_\alpha(\rho)=c_1\exp\left[-\left(\frac{m_\alpha}{m_e}(E_\alpha-\epsilon_\alpha)\right)^{1/2}\rho\right]+c_2\exp\left[+\left(\frac{m_\alpha}{m_e}(E_\alpha-\epsilon_\alpha)\right)^{1/2}\rho\right]. \tag{5.8}$$

In order to prevent $\phi_\alpha(\rho)$ becoming infinite as $\rho\to\infty$, we set $c_2=0$, so that

$$\frac{1}{\phi_\alpha(\rho)}\frac{d\phi_\alpha(\rho)}{d\rho}\to-\left(\frac{m_\alpha}{m_e}(E_\alpha-\epsilon_\alpha)\right)^{1/2}\rho \quad \text{as } \rho\to\infty. \tag{5.9}$$

VI. CALCULATION OF THE TOTAL ENERGY OF THE SYSTEM

The total energy $E[n_e,n_h]$ of the system can be obtained after solving the Kohn-Sham equations given in Eq. (4.4). This gives

$$E[n_e,n_h]=\sum_{\alpha=e,h}\epsilon_\alpha-\tfrac{1}{2}\sum_{\alpha=e,h}\sum_{\beta=e,h}\int d\mathbf{r}\,d\mathbf{r}'u_{\alpha\beta}(\mathbf{r}-\mathbf{r}')\times n_\alpha(\mathbf{r})n_\beta(\mathbf{r}')+E_{\mathrm{xc}}[n_e,n_h]-\sum_{\alpha=e,h}\int d\mathbf{r}\,n_\alpha(\mathbf{r})V_{\mathrm{xc},\alpha}[n_e,n_h], \tag{6.1}$$

However, certain difficulties with this form arise in its conversion into a computational routine. A discussion of these problems, and how they can be overcome, is given below.

The processes described below are repeated by comparing new eigenvalues with those obtained on the previous pass through the procedure, until the results are identical to within a specified accuracy. For a quantitative test of convergence, it is simpler to examine the eigenvalue rather than the eigenvector while ensuring that the eigenvectors are also self-consistent.

A. Initial functions

The self-consistent procedure requires an initial form of the wave function for the first solution to the Kohn-Sham equation (4.4). Therefore, it would at first sight appear sensible to select an analytical function which mimics some anticipated features of the real wave function. However, in order to avoid spurious results and instabilities in the iterative procedure, we found that a more reliable technique was to take the initial function $\phi_\alpha(\rho)=0$, implying that there is no interaction between the particles and the system is merely an electron bound to an impurity center. In addition to stabilizing the results, this procedure had the added advantage that the energy values produced by the first iteration correspond to the binding energy of a D^0 center in a QW, for which accurate values are well known (e.g., Pang and Louie[19] and Xia and Quinn[15]). The disadvantage of taking a zero-valued initial function is that it increases the computation time as at least two iterations are required before a realistic wave function is produced. However, it has been found that this lengthening in the computation time was in-

significant relative to the total time necessary to allow the Kohn-Sham energy levels to converge.

B. Calculation of the effective potential

The form of the effective potential $\nu_{\mathrm{eff},\alpha}(\rho)$ is determined from Eqs. (3.3) and (4.5). Inspection of Eq. (3.3) confirms that two of the terms in the effective potential (the interparticle Coulomb interaction and the exchange-correlation interaction) depend upon the densities $n_\alpha(\mathbf{r})$, and hence upon the particle wave functions $\phi_\alpha(\rho)$. In principle, the calculation of the effective potential is a straightforward example of numerical quadrature. The interparticle Coulomb term is evaluated by use of the well-known general expansion in terms of associated Legendre functions P_l^m

$$\frac{1}{|\mathbf{r}-\mathbf{r}'|}=\sum_{k=0}^{\infty}\sum_{m=-k}^{k}\frac{(k-|m|)!}{(k+|m|)!}\frac{r_a^k}{r_b^{k+1}}P_k^{|m|}(\cos\,\theta_1)\times P_k^{|m|}(\cos\,\theta_2)\exp[im(\phi_1-\phi_2)], \tag{6.2}$$

where r_a is the smaller of $|\mathbf{r}|$ and $|\mathbf{r}'|$, and r_b is the larger of the two. $\{\theta_1,\phi_1\}$ and $\{\theta_2,\phi_2\}$ are the polar angles for $\mathbf{r}$ and $\mathbf{r}'$, respectively. The above expression can be simplified slightly. The last term contributes only if the exponent is zero, and therefore only the $m=0$ term is retained in the second sum. The sum over k must be restricted to a finite number of terms for the computation. As the above sum converges quickly, only a small number of terms need to be retained. The second Hartree term is an integral of the form

$$\int \xi_\alpha^2(z)\left[\sum_{\beta=e,h}\int d\mathbf{r}'\,u_{\alpha\beta}(\mathbf{r}-\mathbf{r}')n_\beta(\mathbf{r}')\right]dz. \tag{6.3}$$

Although this term can be determined accurately, the process involved is particularly time consuming as the integral must be evaluated several thousand times during each evaluation. Therefore, we will evaluate the exact form of the Hartree term at 100 points covering the range of the integration process. A function will then be fitted to these points to represent the interparticle interaction. Thorough examination of this term has shown that the Hartree effective potential is quite smooth, and therefore that the fitting will be unlikely to cause an appreciable inaccuracy in the energy evaluation. The other terms in the effective potential (the particle interaction with the impurity center and the Wunsche-Henneberger exchange-correlation potential) are found readily using expressions (3.3), (3.14), and (3.15).

C. Solution of the electron Kohn-Sham equation

The Kohn-Sham equation (4.4) is a second-order eigenvalue equation. This problem is specified by the form of the electron effective potential $\nu_{\mathrm{eff},e}(\rho)$, and by the boundary conditions on the electron wave function $\phi_e(\rho)$ given by Eqs. (5.6) and (5.9). A shooting method is used to solve Eq. (4.4) and to determine the electron eigenfunction $\phi_e(\rho)$ and the eigenvalue ϵ_e over the semi-infinite range $0\leqslant\rho\leqslant\infty$. It is necessary to find a way of representing this by a realistic finite range. We must exclude $\rho=0$ to prevent singularities in the potential occurring due both to the Coulomb interaction with the impurity center, and to the $1/4\rho^2$ term. The asymptotic form of the eigenfunction as $\rho\rightarrow 0$ is imposed at a sufficiently small value of ρ such that the latter term dominates; inspection of the equation reveals that $\rho\sim 10^{-6}$ (in dimensionless units) is a suitable value. For the right-hand boundary value, we simply take an arbitrarily large value of ρ such that the nonconstant terms of the potential have all decayed to a negligible value. Inspection shows that $\rho=20$ is a suitable value.

As mentioned above, the eigenfunction $\phi_e(\rho)$ is calculated as a series of values at a set of lattice points. However, for the succeeding iterations, values of this function are required to generate the potential in the Kohn-Sham equations. In general, the points at which the potential will be evaluated differ from the lattice points of the eigenfunction. Therefore, it is necessary to fit a function to the values given for the eigenfunction $\phi_e(\rho)$. An interpolating spline is chosen as a suitable compromise between fitting the points exactly, and being a smooth function over the range of integration.

D. Solution of the hole Kohn-Sham equation

The solution of the single-particle equation for the hole equation (4.4) is treated by a similar process to that of the electron. The hole equation may be solved by repeating the calculation for the electron with a different form of the boundary conditions described by Eqs. (5.6) and (5.9). However, the entire iteration procedure has been accelerated by using the electron eigenfunction from the previous stage. This will affect the effective potential. Hence this latter stage consists of the same type of procedure as above, but with the updated form of the electron wave function $\phi_e(\rho)$.

E. Calculation of the binding energy

In order to calculate the binding energy, the total energy $E[n_e,n_h]$ of the system is first evaluated by the simple quadrature process using Eq. (6.1). The binding energy E_{XD} is

$$E_{XD}=E(D^0)+E(X)-E[n_e,n_h], \tag{6.4}$$

where $E(D^0)$ is the ground state energy of the neutral impurity as given by the electron eigenvalue on the first iteration of the calculation when the interparticular forces are disregarded. $E(X)$ is the ground-state energy of the free exciton in a single quantum well. To determine this, it is appropriate to use the numerical calculation of Ref. 20, as it is based on very similar approximations to those used in our calculations.

VII. RESULTS

Figure 2 shows our calculated and our experimental values of E_{XD} as a function of the well width. The impurity is located at the mid point of a GaAs/$Ga_{1-x}Al_x$As single QW for $x=0.33$, which corresponds to the value used in the experiments described in Sec. II. The figure also includes the experimental results of Ref. 3 and the theoretical calculations of Refs. 4–6. The improvement of our model over previous approaches is very clear, even allowing for the different values of x used in the other models. First, our calculated results are closer to the experimental points than any of the previous approaches. Second, our approach is the only one to predict

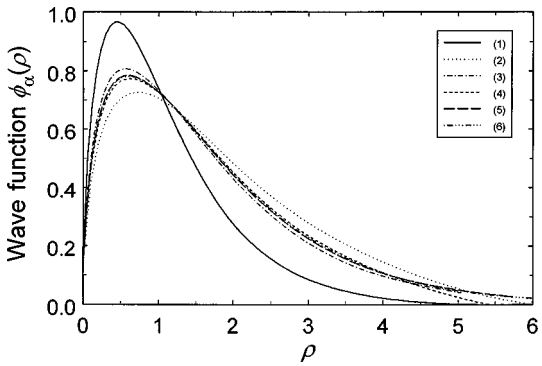

FIG. 3. The first six iterations in the calculation of the electron wave function (as labeled in the key). The first iteration does not include the interparticle effects, but succeeding calculations include increasingly accurate approximations for these effects.

TABLE I. The convergence of the electron eigenvalue for the first ten iterations for a QW of width $d=100$ Å and with $x=0.33$.

Iteration number	Electron eigenvalue
1	−1.977
2	−0.425
3	−0.763
4	−0.632
5	−0.679
6	−0.660
7	−0.668
8	−0.665
9	−0.666
10	−0.666

the observed maximum in E_{XD} for a well width of about 100 Å. Our predicted results for well widths above 100 Å decrease more rapidly with well width than is observed experimentally. However, the agreement between our predicted variation and that observed experimentally is at least as good as that of the previous theoretical approaches, for which the dependence on d is either too rapid (Ref. 4) or too slow (Refs. 5 and 6). Also, the absolute values for the binding energy obtained in our calculations are closer to the experimental data than those of the other approaches.

It is instructive to investigate the convergence of the eigenvalues and eigenfunctions predicted by our method. Figure 3 illustrates the convergence of the electron wave function $\phi_\alpha(\rho)$ as the calculation progresses. The first iteration gives the electron wave function for a D^0 center; the terms in the potential are then calculated using this function to derive a better approximation to the true wave function. This process is repeated at each iteration. Qualitative self-consistency in the wave function occurs rapidly, and the result from the fourth iteration is already close to the final function. However, there is no clear method for us to judge the quantitative convergence of the *eigenfunction* and a better test lies with the *eigenvalue* ε_α. If the process is self-consistent, we should expect to find convergence in the values of ε_α at each iteration; this was indeed observed. Once the eigenvalues have converged, we may compare the eigenfunctions from different stages of the calculation to check that self-consistency has truly occurred. However, it is a slower process for the eigenvalue to converge than for the eigenfunction. As an example of the convergence, we give the electron eigenvalue for $d=100$ Å in Table I. Typically, it requires 20 iterations until a consistent value of the electron eigenvalue can be obtained to four decimal places. A similar number of iterations are required for the hole eigenvalue to converge. Thus at least 40 iterative stages are required in the complete calculation for each well width.

VIII. CONCLUSIONS

The aim of this paper has been to present a more coherent picture of the behavior of the D^0X center in GaAs/$Ga_{1-x}Al_x$ QW's from both experimental and theoretical points of view. Previous experimental investigations by Reynolds *et al.*[3] of the variation of the exciton binding energy with well width (for samples with 100-Å barriers) suggested that there is a maximum in the exciton binding energy E_{XD} at a well width of around 100 Å. However, no other investigations have obtained this result, as insufficient samples have been studied. Hence we have undertaken a comprehensive set of experiments to probe the variation of E_{XD} with well width. These results confirm the existence and position of the maximum obtained by Reynolds *et al.*[3] We have also investigated the variation of the binding energy with impurity doping position.

No theoretical model exists that predicts a maximum in E_{XD} at or anywhere close to 100 Å. Therefore, we have developed a theoretical approach that predicts such a maximum in E_{XD}. The approach chosen is based on an adaptation of density-functional theory. Although density-functional approaches have been applied previously to model excitons in bulk semiconductors[10–14] and the D^- center in a QW, this is the first time (to our knowledge) that such an approach has been used to study excitons in a QW. The model presented here has been shown to give a much closer agreement with the available experimental data than previous theoretical models.[4–6] In particular, it correctly predicts the observed maximum in E_{XD}. Moreover, both the position of the maximum and the actual numerical values obtained for the binding energy are in good agreement with the experimental observations.

The close fit to the experimental points was achieved because a form of the Hamiltonian with corrections which included both exchange and correlation effects was used. Kleinman[5] used an approximate model potential and a two-dimensional approach to mimic the interparticle Coulomb potential. Liu and Kong[4] used a variational procedure with no explicit inclusion of exchange or correlation effects. Consequently, these two methods underestimate the binding energy. Haufe[6] used a variational procedure within a density-functional formalism, and so was able to include exchange and correlation energies and thus predict a higher binding energy. However, the clear maximum in the binding energy at a well width observed experimentally of around 100 Å was not obtained in this approach.

*URA CNRS number 1793.
†Deceased.

[1] Y. Nomura, K. Shinozaki, and M. Ishii, J. Appl. Phys. **58**, 1864 (1985).
[2] X. Liu, A. Petrou, B. D. McCombe, J. Ralston, and G. Wicks, Phys. Rev. B **38**, 8522 (1988).
[3] D. C. Reynolds, C. E. Leak, K. K. Bajaj, C. E. Stutz, R. L. Jones, K. R. Evans, P. W. Yu, and W. M. Theis, Phys. Rev. B **40**, 6210 (1989).
[4] J.-J. Liu and X.-J. Kong, Phys. Rev. B **55**, 1349 (1997).
[5] D. Kleinman, Phys. Rev. B **28**, 871 (1983).
[6] A. Haufe, Solid State Commun. **67**, 899 (1988).
[7] M. J. Pye, C. A. Bates, J. L. Dunn, A. Vasson, A.-M. Vasson, J. Leymarie, and D. Boffety, in *23rd International Conference on the Physics of Semiconductors (Berlin, Germany)*, edited by M. Scheffler and R. Zimmermann (World Scientific, Singapore, 1996), pp. 2007–10.
[8] P. Hohenberg and W. Kohn, Phys. Rev. **136**, 864 (1964).
[9] W. Kohn and L. J. Sham, Phys. Rev. **140**, 1133 (1965).
[10] Y. C. Chang and T. C. McGill, Phys. Rev. B **25**, 3963 (1982).
[11] H. B. Shore and R. S. Pfeiffer, in *Proceedings of the 14th International Conference on the Physics of Semiconductors, Edinburgh*, edited by B. L. H. Wilson, Inst. Phys. Conf. Ser. No. 43 (Institute of Physics, Bristol, 1979), p. 627.
[12] H.-J. Wunsche and K. Henneberger, Phys. Status Solidi B **91**, 331 (1979).
[13] H. J. Muller and H. J. Wunsche, Phys. Status Solidi B **124**, 747 (1984).
[14] R. S. Pfeiffer and H. B. Shore, Phys. Rev. B **25**, 3897 (1982).
[15] X. Xia and J. J. Quinn, Phys. Rev. B **46**, 12 530 (1992).
[16] N. W. Ashcroft and N. D. Mermin, *Solid State Physics* (Holt, Rinehart and Winston, New York, 1976).
[17] H.-J. Wunsche, V. E. Khartsiev, and K. Henneberger, Phys. Status Solidi B **85**, K53 (1978).
[18] J. P. Perdew and A. Zunger, Phys. Rev. B **23**, 5048 (1981).
[19] T. Pang and S. G. Louie, Phys. Rev. Lett. **65**, 1635 (1990).
[20] R. L. Greene, K. K. Bajaj, and D. E. Phelps, Phys. Rev. B **29**, 1807 (1984).